Published in final edited form as:
Cancer. 2013 February 1; 119(3): 563–574. doi:10.1002/cncr.27531.

Regulation of Motility, Invasion and Metastatic Potential of Squamous Cell Carcinoma by 1,25D$_3$

Yingyu Ma, MD, PhD[1], **Wei-Dong Yu, MD**[1], **Bing Su, MD, PhD**[2], **Mukund Seshadri, PhD**[1], **Wei Luo, MD, PhD**[1], **Donald L. Trump, MD**[3], and **Candace S. Johnson, PhD**[1,*]

[1]Department of Pharmacology and Therapeutics, Roswell Park Cancer Institute, Buffalo, NY

[2]Department of Cancer Genetics, Roswell Park Cancer Institute, Buffalo, NY

[3]Department of Medicine, Roswell Park Cancer Institute, Buffalo, NY

Abstract

BACKGROUND—1,25D$_3$, the active metabolite of vitamin D, has been shown to exhibit broad spectrum anti-tumor activity in xenograft animal models. However, its activity against metastatic disease has not been extensively investigated.

METHODS—Squamous cell carcinoma (SCC) or 1,25D$_3$-resistant variant SCC-DR cells were treated with 1,25D$_3$. Actin organization was examined by immunofluorescence assay. Cell migration was assessed by "wound" healing and chemotactic migration assay. Cell invasion was assessed by Matrigel-based invasion assay and i*n situ* zymography. MMP-2 and MMP-9 expression and secretion was examined by immunoblot analysis and ELISA, respectively. E-cadherin expression was assessed by flow cytometry, immunoblot analysis and immunohistochemistry. Knockdown of E-cadherin was achieved by siRNA. Experimental metastasis mouse model was done by intravenous injection of tumor cells. Lung tumor development was assessed by magnetic resonance imaging, gross observation and histology.

RESULTS—SCC cellular morphology and actin organization were altered by 10 nM of 1,25D$_3$. 1,25D$_3$ inhibited SCC cell motility and invasion, which was associated with reduced expression and secretion of MMP-2 and MMP-9. 1,25D$_3$ promoted the expression of E-cadherin. These findings were not observed in SCC-DR cells. Knock down of E-cadherin rescued 1,25D$_3$-inhibited cell migration. Intravenous injection of SCC or SCC-DR cells resulted in the establishment of extensive pulmonary lesions in saline-treated C3H mice. Treatment with 1,25D$_3$ resulted in a marked reduction in the formation of lung tumor colonies in animals injected with SCC but not SCC-DR cells.

CONCLUSIONS—1,25D$_3$ suppresses SCC cell motility, invasion and metastasis, partially through the promotion of E-cadherin-mediated cell-cell adhesion.

Keywords

1; 25D$_3$; SCC; E-cadherin; motility; invasion; metastasis

Corresponding author: Candace S. Johnson, Elm and Carlton Streets, Roswell Park Cancer Institute, Buffalo, NY 14263. Phone: 716-845-8300; Fax: 716-845-1258; candace.johnson@roswellpark.org.

Financial disclosures: There are no financial disclosures from any authors.

INTRODUCTION

Vitamin D is a secosteroid hormone that regulates calcium homeostasis and bone mineralization, as well as a number of other physiological activities.[1] 1α, 25-dihydroxyvitamin D ($1,25D_3$), the active metabolite of vitamin D, has shown broad spectrum anti-tumor activities in numerous preclinical studies.[2–7] $1,25D_3$ exerts growth inhibitory effects by a variety of mechanisms including the induction of apoptosis, cell cycle arrest and differentiation in cancer cells. We have previously demonstrated that $1,25D_3$ inhibits the growth of murine squamous cell carcinoma (SCC) cell line SCCVII/SF *in vitro* and *in vivo*.[5, 8, 9] Apoptosis contributes to this growth inhibition, since $1,25D_3$ induces caspase 3 activation and PARP cleavage in SCC cells.[9] In addition, we have shown that $1,25D_3$ enhances paclitaxel, gemcitabine, cisplatin, and carboplatin-mediated antitumor activities.[10–12] However, the activity of $1,25D_3$ against SCC metastasis has not been extensively studied.

Metastasis is a complex process which involves a series of steps including the initial detachment of cells from the primary tumor, local invasion of the basement membrane, intravasation and survival in the circulation, extravasation, invasion and survival and proliferation in a distant site.[13] Failure of any single step will lead to the suppression of systemic metastasis formation. $1,25D_3$ or its analogs may affect these crucial steps. Sung and Feldman showed that $1,25D_3$ inhibits prostate cancer cell migration and adhesion by down-regulation of integrins.[14] Bao and Lee reported that $1,25D_3$ inhibits prostate cancer cell invasion by suppressing the expression of MMP-9 and cathepsins.[15] However, the mechanisms for the regulation of cell motility and invasion remain unclear. Conversely, vitamin D deficiency promotes cancer cell growth in several metastasis models. In diet-induced vitamin D deficient mice, the growth of human breast cancer cells, injected into the tibia of mice, was enhanced and larger osteolytic lesions was seen in comparison to those observed in vitamin D sufficient mice.[16, 17] Similarly, prostate cancer cell growth in bone was enhanced in vitamin D deficient mice.[18] These observations suggest that $1,25D_3$ may play a role in tumor metastasis by multiple regulatory pathways and promote our investigation.

In the current study, we investigate the role of $1,25D_3$ in the modulation of the morphology and behavior of SCC and SCC-DR cells. The effect of $1,25D_3$ on cell motility and invasion is evaluated. We study the role of E-cadherin mediated cell-cell adhesion in the regulation of SCC cell motility by $1,25D_3$. Furthermore, the *in vivo* activity of $1,25D_3$ in suppressing lung colony formation following intravenous injection is evaluated.

MATERIALS AND METHODS

Materials

$1,25D_3$ (Hoffmann-LaRoche, Nutley, NJ) was reconstituted in 100% ethanol (ETOH) and stored, protected from light, under nitrogen gas at −70°C. Anti-MMP-2 and anti-MMP-9 were from Biomol (Farmingdale, NY). Anti-E-cadherin was from Cell Signaling Technology (Beverly, MA). Anti-actin was from Calbiochem (San Diego, CA).

Cell culture and tumor model system

Murine SCC cells (SCCVII-SF) tumor model and SCC cells were used as described previously.[19] $1,25D_3$-resistant SCC-DR cells were generated by continuously culturing SCC cells in media containing 10 nM of $1,25D_3$ as described previously.[20] SCC cells were maintained in 6–10 weeks old female C3H/HeJ mice purchased from Jackson Laboratory (Bar Harbor, ME). The mice protocols used were approved by the Roswell Park Cancer Institutional Animal Care and Use Committee.

Indirect immunofluorescence assay

SCC or SCC-DR cells were plated on glass coverslips and treated with ETOH or 10 nM $1,25D_3$ for 48 h, washed with PBS, fixed with 60% Acetone/3.7% paraformaldehyde in PBS, and blocked with 25% normal goat serum at room temperature. Actin filaments were stained with rhodamine-labeled phalloidin (Sigma; 1:500), and nuclei were stained with DAPI (1:1000, Invitrogen) for 1 h. Fluorescent images were captured using Nikon TE2000-E inverted microscope equipped with Roper CoolSnap HQ CCD camera.

"Wound" healing assay

A confluent monolayerof SCC cells was cultured overnight and a scratch was introduced with a pipette tip and images of cell migration into the wound werecaptured at 0, 24 and 48 h using a light microscope.

Chemotaxis migration assay

Chemotactic migration activity was measured by Boyden-chamber assay using BD BioCoat Control Inserts. SCC or SCC-DR cells were plated in insert chambers in serum-free RPMI1640. The lower chambers were filled with RPMI1640 with 5% FBS. After 16 h of incubation, cells did not migrate were removed from the upper chambers with a cotton swab, and cells that had migrated through the pore membrane were identified by Diff-Quik® Stain Set (Dade Behring, Newark, DE), examined and counted under a bright field microscopy.

Invasion assay

The invasion activity was measured by Boyden-chamber assay using BD BioCoat Matrigel Invasion Chambers as in the chemotaxis migration assay except for a longer incubation time of 48 h. The results are expressed as follows: % invasion index = (the number of cells migrating through the collagen-coated membrane/the number of cells migrating through the uncoated control membrane) × 100.

In situ zymography

Glass coverslips were coated with 0.2 mg/ml Oregongreen® 488-conjugated gelatin (Invitrogen),cross-linked in 0.5% glutaraldehyde for 15 min at 4°C, and incubatedwith 5 mg/ml $NaBH_4$ for 3 min. The coverslips were then sterilized with 70% ETOH for 15 min and incubated in serum-free media for 1 h at 37°C. SCC or SCC-DR cells were plated on coated coverslips, treated with ETOH or 10 nM $1,25D_3$, and incubated at 37°C for 24 h and processed by Fluorescence Microscopy procedures.

Flow cytometry

SCC or SCC-DR cells treated with ETOH or 10 nM of $1,25D_3$ for 48 h were harvested with Typsin-EDTA, blocked with 3%BSA/PBS for 1 h and incubated with IgG isotype control or rabbitanti-E-cadherin 5 μg/ml for 1 hat room temperature and then washed twice with PBS. Samples were stained with PE-conjugated goat anti-rabbit secondary antibody for 1 h. Flow cytometric analysis wasperformed on a Becton Dickinson FACScan flow cytometer, and data analyzed with FCS Express (De Novo Software, Los Angeles, CA).

Immunoblot analysis

Cell lysates were prepared and immunoblot analysis performed as described previously.[5]

ELISA

The levels of MMP-2 (AbCam, Cambridge, MA) and MMP-9 (R&D systems, Minneapolis, MN) secreted to the culture media were assessed by the ELISA kits according to the manufacturers' instructions.

Immunohistochemistry

For immunohistochemistry studies, SCC cells (4.5×10^5) were inoculated s.c. into the flank of C3H mice. Mice were treated for 3 d with single, daily i.p. injectionsof saline or 0.625 μg/mouse of $1,25D_3$ when tumors were palpable. On day 4, tumor tissues were harvested, fixed in 10% formalin, embedded in paraffin and sectioned at 5 microns. Slides were de-parafinized in xylene, rehydrated, and incubated with 10% normal goat serum followed by avidin/biotin block (Vector Labs, Burlingame, CA) to block non-specific binding. Anti-E-Cadherin antibody (1:500, BD, Cat #610181) was incubated for 30 min at room temperature, followed by biotinylated horse anti-mouse secondary antibody (Vector Labs) for 15 min. ABC reagent (Vector Labs) was then applied for 30 min. To reveal endogenous peroxidase activity, slides were incubated with DAB substrate (Dako, Carpinteria, CA) for 5 min and counterstained with Modified Harris Hematoxylin (Richard-Allan Scientific, Kalamazoo, MI) for 20 sec. Slides were dehydrated and cover slips were mounted with Permount (Fisher, Pittsburgh, PA).

siRNA transfection

siGENOME siRNAs specific for E-cadherin, non-specific siRNA (siRNA-NS), and DHarmaFECT 1 transfection reagent were purchased from Dharmacon (Lafayette, CO). SCC cells were transfected with 50 nM of siRNA-NS or siRNA-E-cadherin for 24 h using DharmaFECT 1 following the manufacturer's protocol.

Magnetic resonance imaging of lung metastasis

Experimental MRI studies were performed using 4.7 T/33-cm horizontal bore magnet (GE NMR Instruments, Fremont, CA) incorporating a removable gradient coil insert (G060; Bruker Medical Inc., Billerica, MA) generating maximum field strength of 950 mT/m and a custom-designed 35-mm RF transmit-receive coil. Induction and maintenance of anesthesia during imaging was achieved by inhalation of 2–3% Isoflurane in oxygen (Abbott Laboratories, IL). Animal body temperature was maintained at 37°C during imaging using an air heater system (SA Instruments Inc., Stony Brook, NY). Animals were placed prone on an MR-compatible sled ((Dazai Research Instruments, Toronto, Canada) within a carrier tube and positioned to ensure placement of the thoracic region of the mice in the isocenter of the magnet. Global shimming was performed at the beginning of imaging to ensure optimal field homogeneity. Preliminary scout images were acquired on the sagittal plane for localization and for determination of subsequent slice prescriptions. Coronal T2-weighted (T2W) images were acquired with the following parameters: FOV = 4.8 × 3.2 cm, matrix (MTX) = 256 × 192, slice thickness = 1.00 mm, TE_{eff} = 41 ms, TR = 2424 ms, no. of averages = 4. A total of 21 slices were acquired across the thoracic region to cover the entire lung area. Axial T2W images were acquired using the same sequence (FOV = 3.2 × 3.2; 25 slices). The duration of imaging session for each animal including induction of anesthesia, positioning and set up was ~20 min. Following image acquisition, raw image sets were transferred to a processing workstation and processed using the medical imaging software, Analyze (AnalyzeDirect, version 7.0; Overland Park, KS). Tumor volumes (mm^3) were calculated from the manually traced tumor area in each acquired slice and the slice thickness.

Ex-vivo quantification of experimental lung metastasis

For experimental metastasis, 10^5 SCC cells or 3×10^5 SCC-DR cells were injected into tailveins of C3H/HeJ mice (6/group). Lung tumor development was monitored by MRI weekly. Mice bearing SCC tumors were sacrificed at 2 weeks and those with SCC-DR tumors were sacrificed at 5–7 weeks post transplantation. The upper trachea was sealed using 4-0 silk and the lungs removed and stained with intratracheally administered 5% (v/v) India ink using blunt end 21G needle; lungs were fixed in Fekete'ssolution (100 ml of 70% alcohol, 10 ml formalin, and 5 ml glacialacetic acid); metastases were scored as surface lesions excludingink.

Sample sizes and statistical considerations

For *in vitro* studies, differences between control and treatment groups were analyzed for statistical significance using two-tailed student's *t*-test. For *in vivo* imaging studies, a total of 29 animals underwent experimental MRI examinations for quantification of pulmonary metastasis. In the first set of studies, 14 animals were injected with SCC cells and assigned to one of three groups: saline (n=8), 0.3 μg $1,25D_3$ (n=3) or 0.6 μg $1,25D_3$ (n=3). Presented in the figure, MRI examinations were performed ~11–15 days post intravenous injection of tumor cells to quantify pulmonary tumor burden. In the second set of studies, 15 animals were injected with SCC-DR cells and treated with saline (n=4) or 0.3 μg $1,25D_3$ (n=6) or 0.6 μg $1,25D_3$ (n=5) and MRI examinations were performed ~40–50 days post injection. Differences in MRI-based tumor volume measurements were analyzed by one-way analysis of variance (ANOVA) with Bonferroni's multiple comparisons test.

RESULTS

$1,25D_3$ modifies SCC cell morphology

To investigate the impact of $1,25D_3$ on the cellular processes involved in metastasis, we first characterized the phenotype of SCC cells by light microscopy. SCC cells normally present a polygonal appearance, as shown in vehicle control ETOH-treated cells (Fig. 1A). However, $1,25D_3$ induced a different phenotype after 48 h. SCC cells were larger and had a flat morphology (Fig. 1A). $1,25D_3$ did not change the morphology of the $1,25D_3$-resistant SCC-DR cells, generated through continuous culture of SCC cells in $1,25D_3$-containing media[20] (Fig. 1A). Cytoskeletal reorganization is essential for changing the cell shapes, cell migration, and other processes.[21] Actin staining revealed a major reorganization of cell cytoskeleton, numerous actin stress fibers were seen throughout cytoplasm of $1,25D_3$-treated SCC cells, while control cells displayed disorganized actin cytoskeleton (Fig. 1B). In contrast, $1,25D_3$ did not change the morphology and actin staining pattern of SCC-DR cells (Fig. 1), indicating the critical role of $1,25D_3$ in cytoskeletal reorganization.

$1,25D_3$ inhibits SCC cell migration

Actin polymerization is a major factor involved in cell migration.[22] Therefore, we next examined the ability of $1,25D_3$ to modify cell motility using the scratch "wound" healing and Boyden chamber-based chemotaxis assays. In the wound healing assay, ETOH-treated SCC cells covered at least 50% of the gap at 24 h and almost the entire damaged area by 48 h (Fig. 2A). In contrast, the scratch was still largely uncovered at 48 h in $1,25D_3$-treated SCC cells (Fig. 2A). SCC-DR cells migrated more slowly than SCC cells, and $1,25D_3$ did not affect the migration rate (Fig. 2A). In the Boyden chamber assay, $1,25D_3$ markedly ($P < .00001$) inhibited the chemotactic migration activity of SCC cells. Interestingly, $1,25D_3$ inhibited migration of SCC-DR cells ($P < .01$), but substantially less than SCC cells (Fig. 2B). These results indicate that $1,25D_3$ suppresses the motility of SCC cells.

$1,25D_3$ inhibits SCC cell invasion

To explore the effect of $1,25D_3$ on the invasiveness of SCC cells, the Matrigel-based invasion chamber assay and in situ gelatin degradation assay were performed. $1,25D_3$ significantly ($P < .01$) reduced the invasion of SCC cells through Matrigel membrance (Fig. 3A). Gelatinase activity (indicating the activity of MMP-2and MMP-9) was assessed by in situ zymography. The ability of SCC cells to degrade matrix in situ was markedly suppressed by $1,25D_3$ treatment, as shown by reduced Oregon green-labeled gelatin degradation area which appears as black holes (Fig. 3B). In contrast, neither the invasiveness nor matrix degradation potential of SCC-DR cells were affected by $1,25D_3$ (Fig. 3A-B). The expression levels of gelatinases MMP-2 and MMP-9 were assessed by immunoblot analysis and markedly reduced expression of both was observed in SCC cells treated with $1,25D_3$ (Fig. 3C). Supporting these findings, the levels of MMP-2 and MMP-9 secreted into cell culture media were reduced by the treatment of 10 or 100 nM of $1,25D_3$ in SCC cells (Fig. 3D).

$1,25D_3$ induces E-cadherin expression in SCC cells

E-cadherin is involved in cell polarity, structure, and invasion. Therefore, we next investigated whether $1,25D_3$-induced morphology and motility changes of SCC cells were associated with changes in E-cadherin expression. $1,25D_3$ markedly induced the expression of membrane E-cadherin in SCC cells as assessed by flow cytometry (Fig. 4A). The expression of E-cadherin was not modified in SCC-DR cells (Fig. 4A). In line with this finding, immunoblot analysis results showed enhanced E-cadherin expression upon $1,25D_3$ treatment in SCC cells (Fig. 4B). To examine whether E-cadherin was modulated *in vivo*, SCC or SCC-DR tumor-bearing mice were treated with $1,25D_3$ for 3 days. Tumors were collected and E-cadherin level was assessed by immunohistochemistry. The treatment with $1,25D_3$ markedly promoted the expression of E-cadherin in SCC tumors but not in SCC-DR tumors (Fig. 4C).

E-cadherin contributes to $1,25D_3$-reduced SCC cell motility

To study whether E-cadherin plays a role in $1,25D_3$-regulated cell migration, siRNA-E-cadherin was used to knockdown E-cadherin expression in SCC cells, as confirmed by flow cytometry (Fig. 5A) and immunoblot analysis (Fig. 5B). Knockdown of E-cadherin promoted SCC cell migration, indicating E-cadherin contributes to SCC motility (Fig. 5C). $1,25D_3$ treatment suppressed migration of control siRNA-NS transfected SCC cells, but to a lesser degree of siRNA-E-cadherin-transfected SCC cells (Fig. 5C). This result indicated that siRNA-E-cadherin rescued SCC cell migration inhibited by $1,25D_3$, which can be seen more easily when migration was normalized to siRNA-NS control (Fig. 5D). Together, these findings suggest that the $1,25D_3$-suppressed SCC cell migration may be due, at least in part, to increased expression of E-cadherin.

$1,25D_3$ inhibits the formation of lung metastases of SCC tumor

Since $1,25D_3$ markedly inhibited SCC cell migration and invasion, we next examined the *in vivo* effect of $1,25D_3$ on metastasis, employing a lung tumor colony formation mouse model. Non-invasive MRI was used to quantify tumor burden in the lungs following intravenous injection of SCC or SCC-DR cells. Coronal and axial T2-weighted images provided adequate contrast for detecting the lesions in relation to the healthy lung parenchyma. In saline-treated control animals injected with SCC cells, multiple bilateral lesions were visible on multislice T2-weighted images (Fig. 6A, *upper left panel*). In contrast, treatment with $1,25D_3$ resulted in a marked reduction ($P < .0001$) in pulmonary tumor nodules (Fig 6A). MRI of animals injected with SCC-DR cells revealed a distinct pattern of tumor formation with large masses visible in the lungs (Fig. 6A, *lower left panel*).

Treatment with $1,25D_3$ did not appear to result in any inhibition of tumor growth in SCC-DR model system. Ex-vivo macroscopic analysis of lungs was performed after intratracheal instillation of India ink permits visualization of lung tumor colonies (Fig. 6B) to validate imaging findings. Consistent with the MRI data, a marked reduction in tumor colonies was seen in $1,25D_3$-treated animals injected with SCC cells compared to saline treated controls. Histological examination of lung tissue sections obtained from saline-treated animals injected with SCC cells revealed extensive regions of normal lung parenchyma replaced by tumor tissue (Fig. 6C). In comparison, lungs excised from animals treated with $1,25D_3$ showed presence of healthy lung tissue with fewer areas of malignant transformation. On the other hand, $1,25D_3$ did not alter the histology of lung tissues obtained from animals injected with SCC-DR cells (Fig. 6C). These results indicate that $1,25D_3$ strongly inhibits the formation of lung tumor colonies following intravenous introduction of SCC cells.

DISCUSSION

There is growing evidence that $1,25D_3$ may have antitumor activity in a number of cancer types including colorectal, breast, prostate, ovarian and skin cancers. In addition to suppressing cancer cell proliferation and apoptosis, $1,25D_3$ affects angiogenesis and tumor metastasis.[5, 23–25] However, the mechanisms for these anticancer effects remain unclear and further investigations are needed.

In this study, we show that $1,25D_3$ modulates the morphology of SCC cells from polygonal to bigger and more flattened shape. Pendas-Franco et al. showed that human breast cancer cell MDA-MB-453 underwent different morphology change upon $1,25D_3$ treatment, from rounded shape to polygonal and flattened.[26] Assembly of actin stress fibers was observed in both studies, indicating a role for $1,25D_3$ in regulating the organization of cytoskeleton, which may lead to changes in cell shape and motility.

Modulation of cell cytoskeleton organization may affect cell motility. Further studies employing “wound” healing assay and chemotactic migration assay demonstrate that $1,25D_3$ inhibits the migration and chemotaxis of SCC cells. The invasiveness of SCC cells is also markedly suppressed by $1,25D_3$, as examined in the Matri-gel Boyden chamber assay and *in situ* zymography, which is a unique and important technique to show the proteolytic activity at specific sites of tissues or cell cultures. This is associated with reduced expression and secretion of MMP-2 and MMP-9 in SCC cells, shown by immunoblot analysis and ELISA, respectively. The mechanisms for $1,25D_3$-mediated inhibition of tumor cell motility are not well understood. $1,25D_3$-reduced invasion of Lewis lung carcinoma cancer cell line LLC-LN7 through matrix-coated membranes, and this effect was associated with decreased protein kinase A activity.[27] Young et al. studied on LLC-LN7 and showed that $1,25D_3$-suppressed tumor cell motility was associated with the inhibition of GM-CSF production.[28] $1,25D_3$ inhibited invasion of prostate cancer cell lines LNCaP, PC-3 and DU145 assessed by Matrigel invasion assay, which was associated with decreased MMP- 9 and cathepsin activity and increased tissue inhibitors of metalloproteinase-1 activity.[15] $1,25D_3$ may play an opposite role in motility in normal cells. Rebsamen et al. noted that enhanced cell motility of benign vascular smooth muscle cells in association with phosphatidylinositol 3-kinase activation.[29] The possible differential regulation of cell motility may be beneficial in cancer treatment since it may spare the normal cells from the adverse effect.

E-cadherin mediates cell-cell adhesion, and the disruption of the strong cell-cell adhesion leads to the invasion and metastasis of tumor cells.[30] Loss of E-cadherin not only causes deregulation of cytoskeleton and loss of cell polarity, but also leads to increased cell motility and invasiveness,[31] possibly because E-cadherin-mediated cell-cell adhesion promotes cell clusters and thus restricts cell motility towards extracellular matrix. Cell-cell adhesion

mediated by E-cadherin is often lost with the development of invasiveness in epithelial cancer.[32] E-cadherin loss may be due to several mechanisms. MicroRNA miR-9 inhibits E-cadherin expression and enhances mammary epithelial cell motility and invasiveness and the silencing of miR-9 in breast cancer cells suppresses lung metastasis in an orthotopic implantation model.[33] E-cadherin may be silenced by DNA hypermethylation around the promoter region in premalignant situations.[34] MMPs can proteolytically cleave and disrupt the function of E-cadherin.[31] Therefore, restoring the function of E-cadherin may inhibit tumor metastasis.

In the current study, we have identified a novel link between $1,25D_3$-induced E-cadherin expression and decreased cell migration. $1,25D_3$ promotes the expression of E-cadherin in SCC cells and tumors, as demonstrated by flow cytometry, immunoblot analysis and immunohistochemistry. E-cadherin induction is VDR-dependent since $1,25D_3$ did not affect E-cadherin level in SCC-DR cells which have defective VDR signaling.[20] In line with our data, another study showed that $1,25D_3$ induced the expression of E-cadherin expression in colon carcinoma cells.[35] We demonstrate for the first time that silencing of E-cadherin by siRNA rescues $1,25D_3$-inhibited SCC cell migration. These data indicate that $1,25D_3$-enhanced E-cadherin expression contributes to $1,25D_3$-mediated inhibition of SCC cell motility.

With the observation that $1,25D_3$ strongly inhibits SCC cell motility and invasion *in vitro*, we next investigated the effect of $1,25D_3$ *in vivo* in an experimental mouse model, in which SCC cells were injected intravenously into mice and tumor growth in lungs was monitored. By *in vivo* MRI, ex-vivo macroscopic and microscopic analyses, we show that $1,25D_3$ markedly suppresses the ability of SCC cells to establish pulmonary metastases. Interestingly, comparing to SCC cells, it takes much longer for SCC-DR cells to form tumor colonies in lungs after being introduced intravenously in mice. And they form fewer colonies than SCC cells. This observation may be due to the fact that SCC-DR cells express higher level of endogenous E-cadherin in comparison to SCC cells, as shown by Flow cytometry and immunoblot analysis, and thus decreased ability in migration and invasion. This experimental metastasis model has intrinsic limitations because cancer cells are introduced directly to the circulation, therefore it can not evaluate the initial metastasis processes when cancer cells need to escape the primary tumor, invade through the basement membrane, migrate and invade through the surrounding tissue and then enter the circulation. Spontaneous metastasis models should be used if feasible.

Supporting our findings, $1,25D_3$ was shown to inhibit metastatic growth in several tumor models. $1,25D_3$ suppressed spontaneous and experimental pulmonary metastasis of B16 mouse melanoma.[25] 22-oxa-$1,25D_3$ reduced the lung colony formation in the intravenous injection model and angiogenesis in the basic fibroblast growth factor-induced angiogenesis model.[36] Vitamin D analog EB1089 suppressed the occurrence of bone metastasis in a breast cancer metastasis model.[37] $1,25D_3$ or 22-oxa-$1,25D_3$ treatment suppressed lung metastasis of Lewis lung carcinoma cells in an intravenous injection mouse model.[36] Although the preclinical models support an anti-metastatic role for $1,25D_3$, further studies are needed to assess the clinical relevance.

In conclusion, we show that $1,25D_3$ modulates SCC cell morphology and actin arrangement. In addition, $1,25D_3$ inhibits SCC cell motility, possibly through the promotion of E-cadherin expression. $1,25D_3$ inhibits the invasiveness of SCC cells, which is associated with decreased expression and secretion of MMP-2 and MMP-9. *In vivo*, $1,25D_3$ suppresses SCC lung metastasis in an experimental model approximating metastasis. Although further mechanistic investigation into the regulation of metastasis by $1,25D_3$ is necessary, the

observed anti-metastatic activity of $1,25D_3$ in multiple preclinical model systems supports its evaluation in the clinical setting.

Acknowledgments

Financial support: This study was supported by NIH/NCI grants CA067267,CA085142 (Johnson, CS), CA095045 (Trump, DL) and utilized core resources supported by NCI P30CA16056 (Trump, DL).

The authors would like to thank Mrs. Rui-Xian Kong for her excellent technical support, Mr. Steve G. Turowski for assistance with MRI studies, Ms. Ellen Karasik for her excellent technical assistance in immunohistochemistry study, and Dr. Pamela A. Hershberger for her critical review of the manuscript.

References

1. Brown AJ, Dusso A, Slatopolsky E. Vitamin D. Am J Physiol. 1999; 277:F157–175. [PubMed: 10444570]
2. Peehl DM, Skowronski RJ, Leung GK, Wong ST, Stamey TA, Feldman D. Antiproliferative effects of 1,25-dihydroxyvitamin D3 on primary cultures of human prostatic cells. Cancer Res. 1994; 54:805–810. [PubMed: 7508338]
3. Zhang X, Li P, Bao J, et al. Suppression of death receptor-mediated apoptosis by 1,25-dihydroxyvitamin D3 revealed by microarray analysis. J Biol Chem. 2005; 280:35458–35468. [PubMed: 16093247]
4. Shabahang M, Buras RR, Davoodi F, et al. Growth inhibition of HT-29 human colon cancer cells by analogues of 1,25-dihydroxyvitamin D3. Cancer Res. 1994; 54:4057–4064. [PubMed: 8033137]
5. McGuire TF, Trump DL, Johnson CS. Vitamin D(3)-induced apoptosis of murine squamous cell carcinoma cells. Selective induction of caspase-dependent MEK cleavage and up-regulation of MEKK-1. J Biol Chem. 2001; 276:26365–26373. [PubMed: 11331275]
6. Colston KW, Berger U, Coombes RC. Possible role for vitamin D in controlling breast cancer cell proliferation. Lancet. 1989; 1:188–191. [PubMed: 2563099]
7. Eisman JA, Barkla DH, Tutton PJ. Suppression of in vivo growth of human cancer solid tumor xenografts by 1,25-dihydroxyvitamin D3. Cancer Res. 1987; 47:21–25. [PubMed: 3024816]
8. McElwain MC, Modzelewski RA, Yu WD, Russell DM, Johnson CS. Vitamin D: an antiproliferative agent with potential for therapy of squamous cell carcinoma. Am J Otolaryngol. 1997; 18:293–298. [PubMed: 9282244]
9. Bernardi RJ, Trump DL, Yu WD, McGuire TF, Hershberger PA, Johnson CS. Combination of 1alpha,25-dihydroxyvitamin D(3) with dexamethasone enhances cell cycle arrest and apoptosis: role of nuclear receptor cross-talk and Erk/Akt signaling. Clin Cancer Res. 2001; 7:4164–4173. [PubMed: 11751517]
10. Hershberger PA, Yu WD, Modzelewski RA, Rueger RM, Johnson CS, Trump DL. Calcitriol (1,25-dihydroxycholecalciferol) enhances paclitaxel antitumor activity in vitro and in vivo and accelerates paclitaxel-induced apoptosis. Clin Cancer Res. 2001; 7:1043–1051. [PubMed: 11309356]
11. Light BW, Yu WD, McElwain MC, Russell DM, Trump DL, Johnson CS. Potentiation of cisplatin antitumor activity using a vitamin D analogue in a murine squamous cell carcinoma model system. Cancer Res. 1997; 57:3759–3764. [PubMed: 9288784]
12. Ma Y, Yu WD, Trump DL, Johnson CS. 1,25D(3) Enhances antitumor activity of gemcitabine and cisplatin in human bladder cancer models. Cancer. 2010; 116:3294–3303. [PubMed: 20564622]
13. Nguyen DX, Bos PD, Massague J. Metastasis: from dissemination to organ-specific colonization. Nat Rev Cancer. 2009; 9:274–284. [PubMed: 19308067]
14. Sung V, Feldman D. 1,25-Dihydroxyvitamin D3 decreases human prostate cancer cell adhesion and migration. Mol Cell Endocrinol. 2000; 164:133–143. [PubMed: 11026565]
15. Bao BY, Yeh SD, Lee YF. 1alpha,25-dihydroxyvitamin D3 inhibits prostate cancer cell invasion via modulation of selective proteases. Carcinogenesis. 2006; 27:32–42. [PubMed: 15987715]
16. Ooi LL, Zhou H, Kalak R, et al. Vitamin D deficiency promotes human breast cancer growth in a murine model of bone metastasis. Cancer Res. 2010; 70:1835–1844. [PubMed: 20160035]

17. Ooi LL, Zheng Y, Zhou H, et al. Vitamin D deficiency promotes growth of MCF-7 human breast cancer in a rodent model of osteosclerotic bone metastasis. Bone. 2010; 47:795–803. [PubMed: 20638491]
18. Zheng Y, Zhou H, Ooi LL, Snir AD, Dunstan CR, Seibel MJ. Vitamin D deficiency promotes prostate cancer growth in bone. Prostate. 2011; 71:1012–1021. [PubMed: 21541977]
19. Hershberger PA, Modzelewski RA, Shurin ZR, Rueger RM, Trump DL, Johnson CS. 1,25-Dihydroxycholecalciferol (1,25-D3) inhibits the growth of squamous cell carcinoma and down-modulates p21(Waf1/Cip1) in vitro and in vivo. Cancer Res. 1999; 59:2644–2649. [PubMed: 10363987]
20. Ma Y, Yu WD, Hershberger PA, et al. 1alpha,25-Dihydroxyvitamin D3 potentiates cisplatin antitumor activity by p73 induction in a squamous cell carcinoma model. Mol Cancer Ther. 2008; 7:3047–3055. [PubMed: 18790784]
21. Schoenenberger CA, Bischler N, Fahrenkrog B, Aebi U. Actin's propensity for dynamic filament patterning. FEBS Lett. 2002; 529:27–33. [PubMed: 12354608]
22. Pollard TD, Borisy GG. Cellular motility driven by assembly and disassembly of actin filaments. Cell. 2003; 112:453–465. [PubMed: 12600310]
23. Mantell DJ, Owens PE, Bundred NJ, Mawer EB, Canfield AE. 1 alpha,25-dihydroxyvitamin D(3) inhibits angiogenesis in vitro and in vivo. Circ Res. 2000; 87:214–220. [PubMed: 10926872]
24. Bao BY, Yao J, Lee YF. 1alpha, 25-dihydroxyvitamin D3 suppresses interleukin-8-mediated prostate cancer cell angiogenesis. Carcinogenesis. 2006; 27:1883–1893. [PubMed: 16624828]
25. Yudoh K, Matsuno H, Kimura T. 1alpha,25-dihydroxyvitamin D3 inhibits in vitro invasiveness through the extracellular matrix and in vivo pulmonary metastasis of B16 mouse melanoma. J Lab Clin Med. 1999; 133:120–128. [PubMed: 9989763]
26. Pendas-Franco N, Gonzalez-Sancho JM, Suarez Y, et al. Vitamin D regulates the phenotype of human breast cancer cells. Differentiation. 2007; 75:193–207. [PubMed: 17288543]
27. Young MR, Lozano Y. Inhibition of tumor invasiveness by 1alpha,25-dihydroxyvitamin D3 coupled to a decline in protein kinase A activity and an increase in cytoskeletal organization. Clin Exp Metastasis. 1997; 15:102–110. [PubMed: 9062386]
28. Young MR, Halpin J, Hussain R, et al. Inhibition of tumor production of granulocyte-macrophage colony-stimulating factor by 1 alpha, 25-dihydroxyvitamin D3 reduces tumor motility and metastasis. Invasion Metastasis. 1993; 13:169–177. [PubMed: 8034438]
29. Rebsamen MC, Sun J, Norman AW, Liao JK. 1alpha,25-dihydroxyvitamin D3 induces vascular smooth muscle cell migration via activation of phosphatidylinositol 3-kinase. Circ Res. 2002; 91:17–24. [PubMed: 12114317]
30. Birchmeier W, Hulsken J, Behrens J. Adherens junction proteins in tumour progression. Cancer Surv. 1995; 24:129–140. [PubMed: 7553658]
31. Makrilia N, Kollias A, Manolopoulos L, Syrigos K. Cell adhesion molecules: role and clinical significance in cancer. Cancer Invest. 2009; 27:1023–1037. [PubMed: 19909018]
32. Cavallaro U, Christofori G. Cell adhesion and signalling by cadherins and Ig-CAMs in cancer. Nat Rev Cancer. 2004; 4:118–132. [PubMed: 14964308]
33. Ma L, Young J, Prabhala H, et al. miR-9, a MYC/MYCN-activated microRNA, regulates E-cadherin and cancer metastasis. Nat Cell Biol. 2010; 12:247–256. [PubMed: 20173740]
34. Yoshiura K, Kanai Y, Ochiai A, Shimoyama Y, Sugimura T, Hirohashi S. Silencing of the E-cadherin invasion-suppressor gene by CpG methylation in human carcinomas. Proc Natl Acad Sci U S A. 1995; 92:7416–7419. [PubMed: 7543680]
35. Palmer HG, Gonzalez-Sancho JM, Espada J, et al. Vitamin D(3) promotes the differentiation of colon carcinoma cells by the induction of E-cadherin and the inhibition of beta-catenin signaling. J Cell Biol. 2001; 154:369–387. [PubMed: 11470825]
36. Nakagawa K, Sasaki Y, Kato S, Kubodera N, Okano T. 22-Oxa-1alpha,25-dihydroxyvitamin D3 inhibits metastasis and angiogenesis in lung cancer. Carcinogenesis. 2005; 26:1044–1054. [PubMed: 15718253]
37. El Abdaimi K, Dion N, Papavasiliou V, et al. The vitamin D analogue EB 1089 prevents skeletal metastasis and prolongs survival time in nude mice transplanted with human breast cancer cells. Cancer Res. 2000; 60:4412–4418. [PubMed: 10969786]

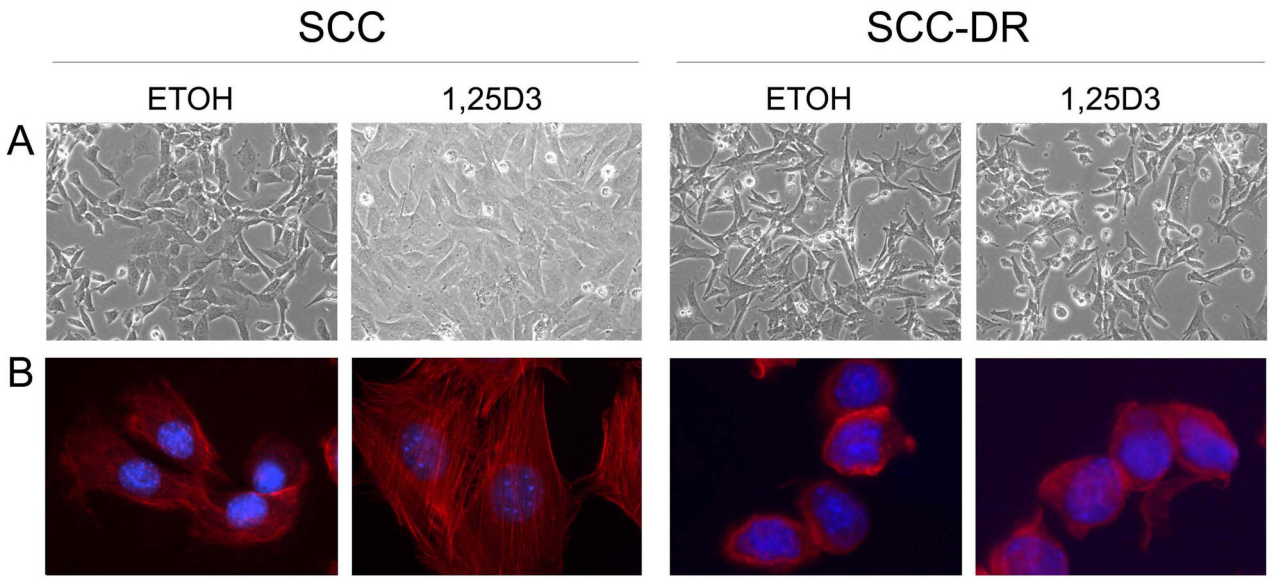

Figure 1.

$1,25D_3$ modifies the phenotype of SCC cells. SCC cells were treated with control ETOH or 10 nM $1,25D_3$ for 48 h. (A) Cell morphologies were examined and photographed with a phase contrast microscope. (× 100) (B) Actin (red) and DAPI (blue) fluorescent staining of SCC cells. Results are representative of three independent experiments.

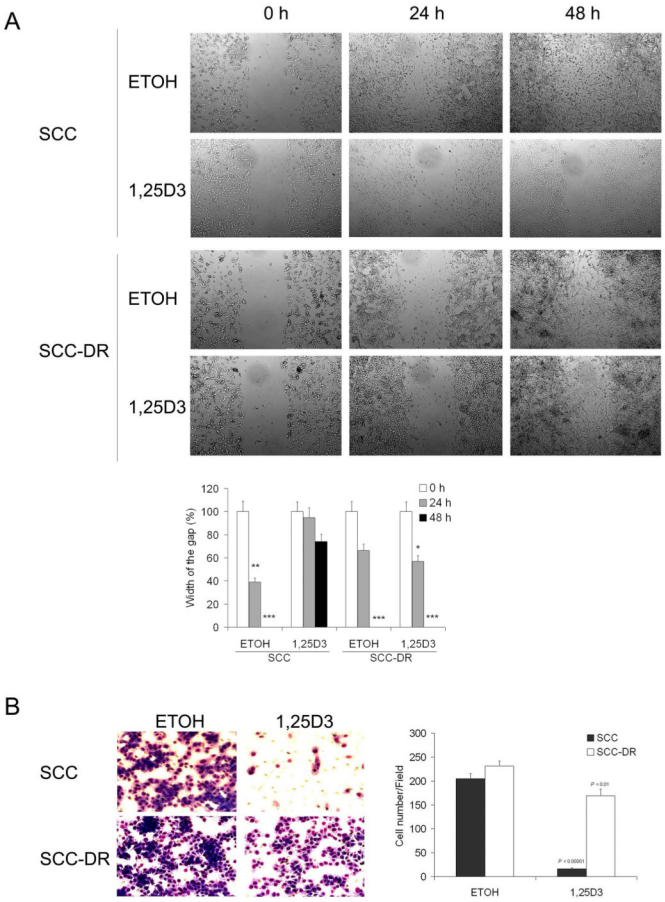

Figure 2.

$1,25D_3$ inhibits SCC cell migration. (A) Wounds were introduced by scratching a monolayer of SCC or SCC-DR cells. Cells were treated with ETOH or 10 nM $1,25D_3$. Migration was monitored by a light microscope at 0, 24 and 48 h. The width of the gaps in three experiments were measured and presented in a bar graph. *, $P < .05$; **, $P < .01$; ***, $P < .001$. (B) SCC or SCC-DR cells were treated with 10 nM $1,25D_3$ for 24 h. Chemotactic migration assay was performed using 8 μm pore modified Boyden chambers with 5% FBS. The cell numbers per field were counted and presented in a bar graph. Results are representative of three independent experiments.

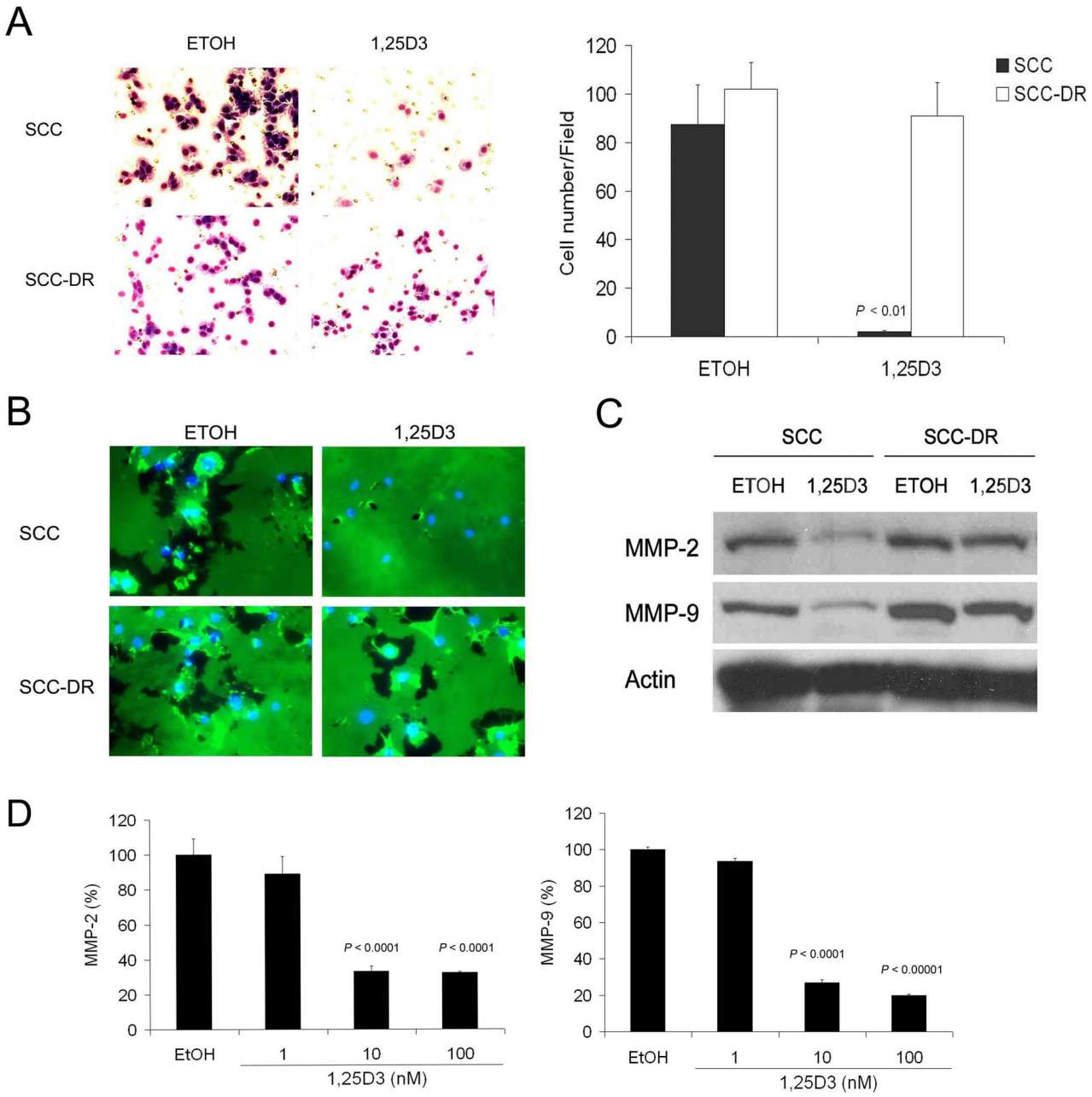

Figure 3.

1,25D_3 inhibits invasion of SCC cells. (A) SCC or SCC-DR cells were treated with ETOH or 10 nM 1,25D_3 for 24 h. Matri-gel based invasion assay was performed using 8 μm pore modified Boyden chambers with 5% FBS. The cell numbers per field were counted and presented in a bar graph. (B) SCC or SCC-DR cells were plated on glass coverslips and treated with ETOH or 10 nM 1,25D_3 for 48 h. *In situ* zymography was performed with Oregongreen® 488-conjugated gelatin. The coverslips were co- stained with DAPI to show nuclei. (C) SCC or SCC-DR cells were treated with ETOH or 10 nM 1,25D_3 for 48 h. MMP-2 and MMP-9 levels were evaluated by immunoblot analysis. Actin was the loading control. (D) SCC or SCC-DR cells were treated with ETOH or 1, 10 or 100 nM 1,25D_3 for

48 h. Culture supernatants were harvested and the levels of MMP-2 and MMP-9 were assessed by ELISA. Results are representative of three independent experiments.

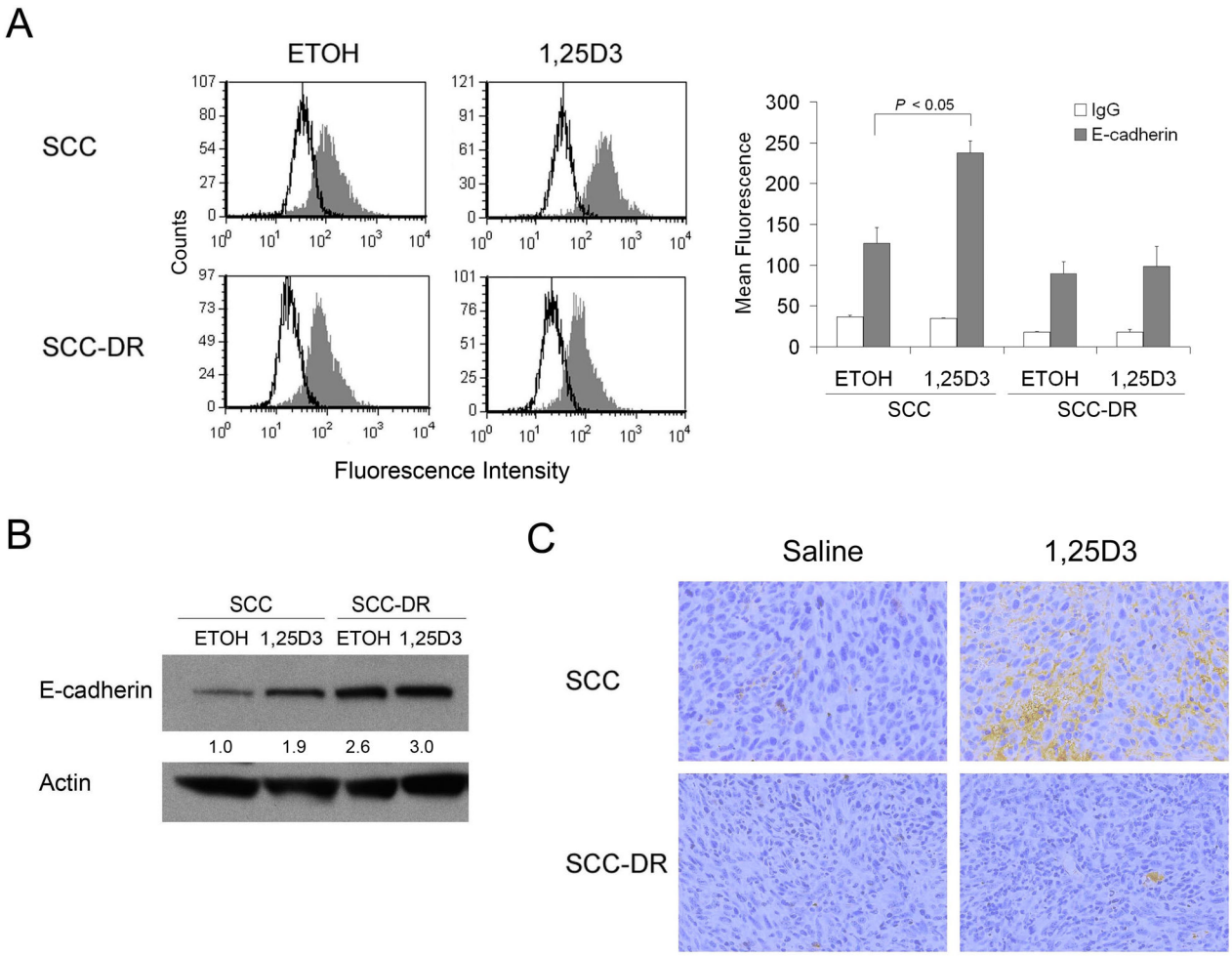

Figure 4.

$1,25D_3$ enhances E-cadherin expression in SCC cells. (A) SCC or SCC-DR cells were treated with ETOH or 10 nM $1,25D_3$ for 48 h. E-cadherin expression level was assessed by flow cytometry. The data were displayed as histograms. Open peak, control IgG; gray peak, E-cadherin. The mean fluorescence was used to quantify the signals and presented in a bar graph. (B) SCC or SCC-DR cells were treated with ETOH or 10 nM $1,25D_3$ for 48 h. E-cadherin expression level was assessed by immunoblot analysis. Actin was the loading control. Densities of E-cadherin bands were presented as fold changes normalized to ETOH control of SCC cells. (C) E-cadherin expression (brown staining) was examined by immunohistochemistry in SCC xenograft tumor tissues in mice treated with saline or $1,25D_3$.

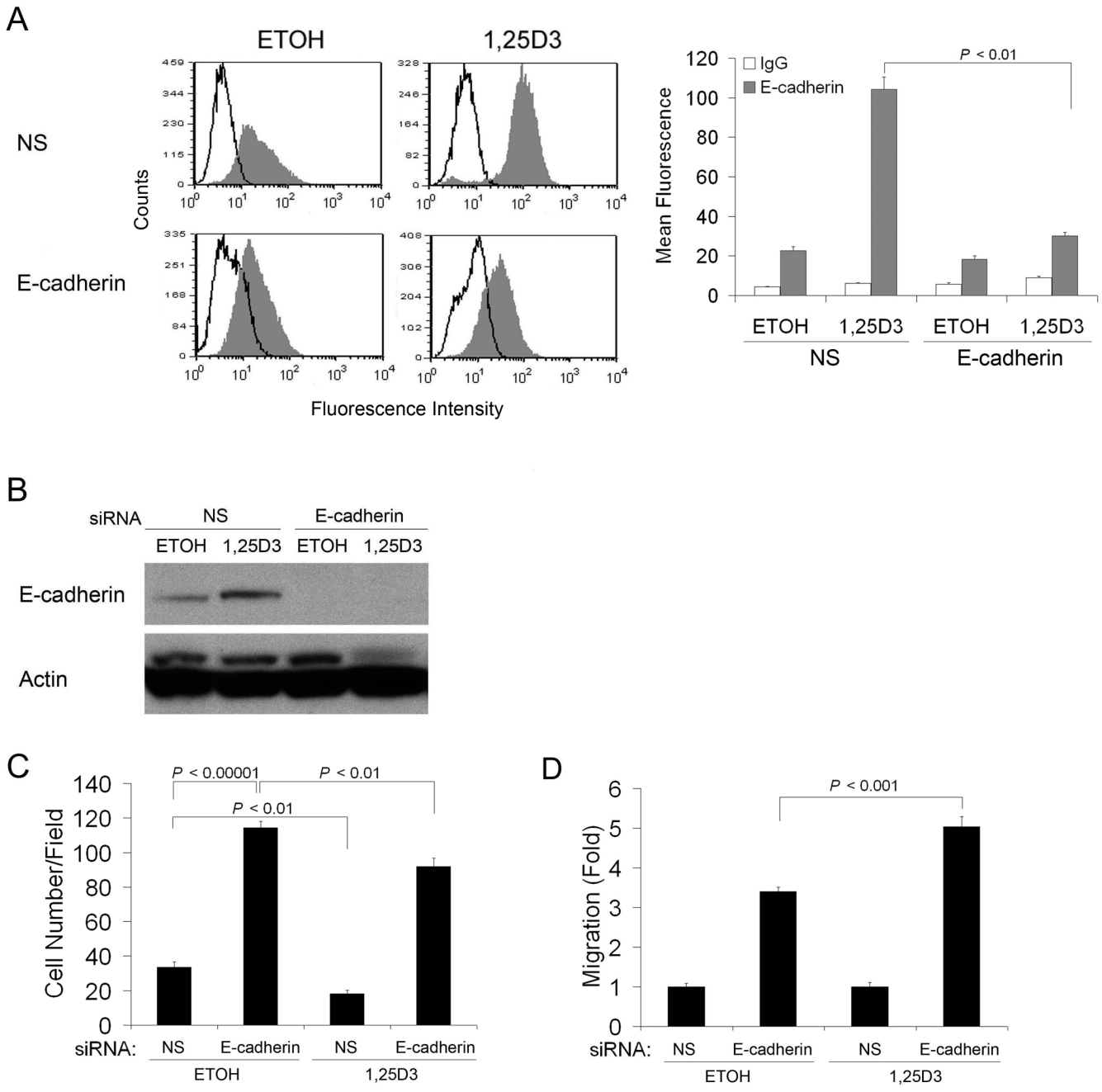

Figure 5.

E-cadherin contributes to $1,25D_3$-reduced SCC cell motility. SCC cells were transfected with non-specific siRNA (NS), or siRNA-E-cadhein for 24 h, followed by the treatment with ETOH or 10 nM $1,25D_3$ for 48 h. (A) E-cadherin expression level was assessed by flow cytometry. Open peak, control IgG; gray peak, E-cadherin. The mean fluorescence was used to quantify the signals and presented in a bar graph. (B) E-cadherin expression was evaluated by immunoblot analysis. Actin was the loading control. (C) si-RNA transfected SCC cells were harvested and subjected to chemotactic migration assay. (D) Migration in (C) was normalized to siRNA-NS transfected groups (1 fold). Results are representative of two independent experiments.

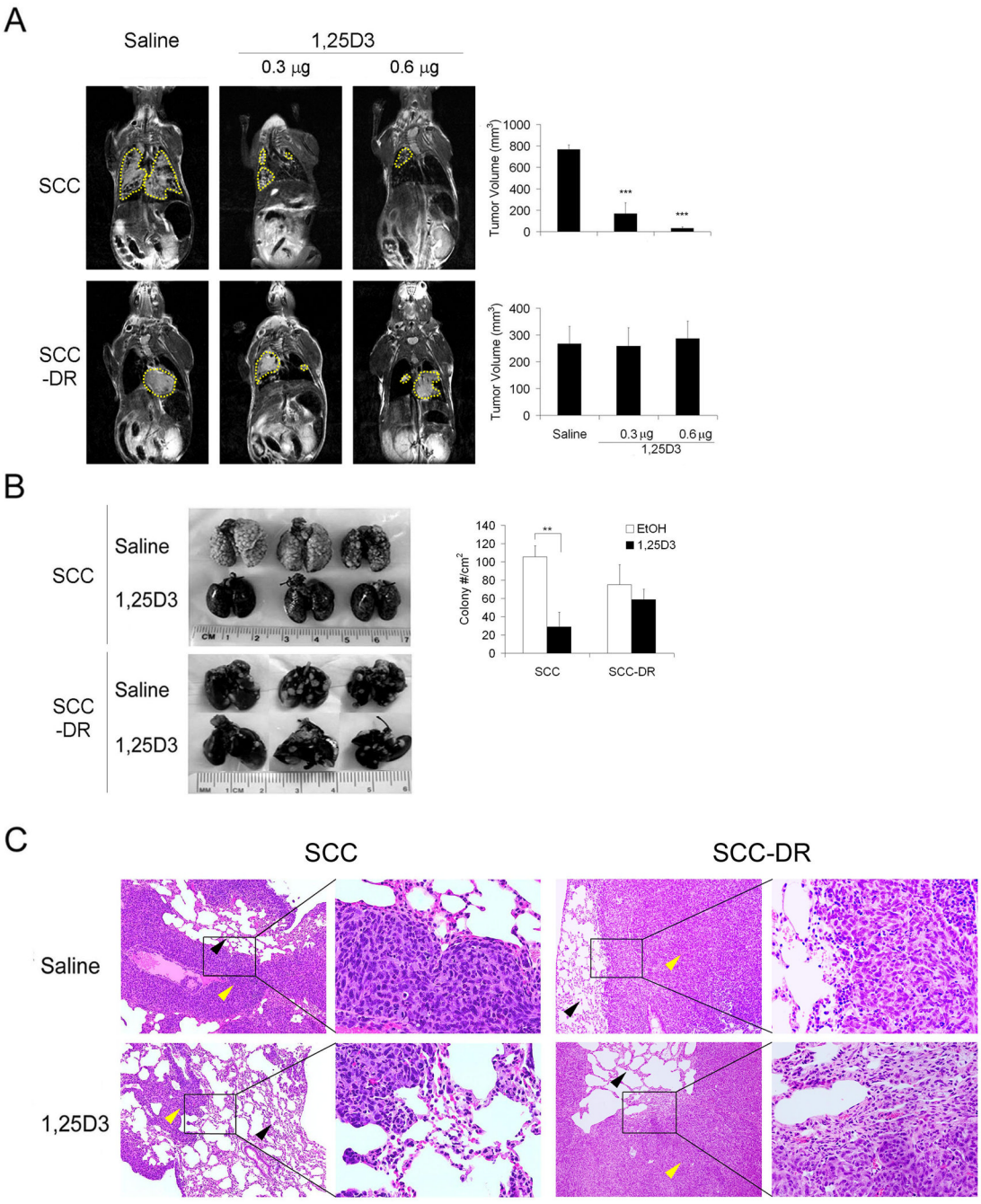

Figure 6.

1,25D_3 inhibits SCC tumor growth in lungs in an experimental metastasis model. SCC or SCC-DR cells were injected through tail vein in C3H/HeJ mice and treated with saline or 1,25D_3 (0.3 or 0.6 μg/mouse) for 3 d. (A) Coronal T2-weighted MR images of saline and 1,25D_3-treated animals along with corresponding bar graphs of tumor volumes. Areas of lung lesions were marked by yellow dashed lines. ***, $P < .0001$. (B) Lungs were harvested, fixed and stained with India ink. Gross images of 3 lungs from each group were presented. Superficial colony counts were presented in a bar graph. **, $P < .001$. (C) Histology was performed on the lungs of saline and 1,25D_3- treated mice injected with SCC or SCC-DR

cells. Representative views of the lung sections were shown. Yellow arrows, tumor; black arrows, lung tissue. (H&E, × 100 and × 400)